Improving GPS Time Transfer Accuracy with the NIST Ionospheric Measurement System

Dick Davis & Marc A. Weiss
National Institute of Standards and Technology Time and Frequency Division
Ken Davies
Space Enviroment Laboratory, National Oceanic and Atmospheric Administration
Gerard Petit
Bureau International des Poids et Mesures

ABSTRACT

The NIST Ionospheric Measurement System (NIMS) uses the GPS P-codes on L1 and L2 without decoding them to measure the ionospheric delay on L1. Data are available every 15 s for all satellites in view. 15 min linear fits to this data are available via modem. The NIMS will also automatically correct time measurements from an NBS/GPS type receiver for the measured ionospheric delay. The accuracy is shown to be a few ns by comparison with the Faraday rotation measurements from the GOES-2 satellite and by computing a time closure around the world with GPS data corrected with ionospheric measurements. The stability of the measurements is about 1 ns at 15 s, and they integrate as white phase noise to about 16 min.

1. INTRODUCTION

The National Institute of Standards and Technology (NIST), Time and Frequency Division, along with many other international time standards laboratories, uses signals from Global Positioning System (GPS) satellites to intercompare clocks at remote locations. Early on, it was found that the C/A code on L1 was adequate to provide time transfer to 10 ns or better. One serious disadvantage of the single frequency C/A receiver is that one must use the broadcast ionospheric model or some independent means of measuring the ionospheric delay. We discuss here the NIST Ionospheric Measurements System (NIMS), its design, its data, and results from applying its data.

The ionosphere is characterized by large variations in both time and space. The total electron content can vary by orders of magnitude from day to night, from summer to winter, and from solar cycle minimum to maximum. It also varies with geographic location [1] and with solar disturbance. A signal from a satellite suffers a delay as it traverses the ionosphere proportional to the total electron content, and inversely proportional to the frequency squared of the carrier. This delay is, of course, in addition to the delay due to the finiteness of the speed of light.

Often the international community accomplishes time transfer using simultaneous measurements of the time a common GPS signal was received at two or more locations. This is called GPS common-view time transfer. In this way, the ionospheric delay in common between two locations cancels, leaving only the differential delay to cause errors in the measurements. The GPS satellites transmit a model of the ionospheric delay at the L1 frequency as part of the C/A code format. This model, being limited to only eight parameters is claimed to be only 50% accurate.

Time transfer using GPS satellites in common view became the primary means for intercontinental comparisons during the 1980's [2]. For most of the

1980's, solar activity was low and the error in the transmitted model of ionospheric delay for common view [3] time transfer was within acceptable limits. However, as we went through the maximum in the approximately 11 year sunspot cycle, the L1 ionospheric delays approached 100 ns for the low angles used for intercontinental time transfer, and the differential delay over such a baseline was a large fraction of this 100 ns. We therefore needed to measure the ionospheric delay rather than use the transmitted model, which at a 50% accuracy could leave large errors.

There are techniques that allow us to measure the differential delay of the P-code between the L1 and L2 frequencies without actually needing to know the codes themselves. One such technique was first developed for measuring the ionosphere in a stand-alone unit by M. Imae of the Communications Research Laboratory (CRL) of Tokyo for the Bureau International des Poids et Mesures (BIPM) [8]. P. MacDoran holds a patent on various codeless techniques and built a codeless GPS geodetic receiver [6].

Cost and security dictated that we consider only such a codeless receiver. The resulting ionospheric measurement system developed by NIST has the following properties. It is self contained with battery backup for the data and internal clock. It makes measurements every 15 s of the L1 ionospheric delay for all satellites in view, with a stability of about 1 ns. The system can be calibrated to obtain an accuracy of a few ns. It directly and automatically interfaces with a NBS/GPS type time transfer receiver. The system can also be used as a stand-alone unit for ionospheric measurements. And it is relatively inexpensive.

We compare the NIMS data with Faraday rotation measurements of the ionosphere using signals from the GOES-2 satellite. We find a general agreement at the level of a few ns, though a number of unknown parameters are discussed. We also compute an around-the-world closure of GPS time transfer measurements comparing the ionospheric measurements with the broadcast model, as well as other parameters. We find that the use of ionospheric measurements made locally at the three sites decrease the fluctuations of the closure and some of the biases, though significant biases are further reduced with the application of the precise ephemeris. The closure is repeated over a period of 273 d, and we find a residual bias of the order of 4 ns.

2. THE IONOSPHERIC DELAY

In traversing the ionosphere a GPS satellite signal of frequency f in Hz suffers a time delay D given by

$$D = 0.1343 \bullet N/f^2$$

in μs where N is the total electron content in a column of 1 m^2 cross section along the ray path. The GPS satellites transmit the same code, called the precise or P-code, on two L-band frequencies: L1 = 154•10.23 MHz = 1.57542 GHz, and L2 = 120•10.23 Mhz = 1.2276 GHz. On a frequency of 1.575 GHz, 1 ns corresponds to an electron content of $1.85 \bullet 10^{16}$ electrons/m^2.

The NIMS recovers the clock which generates the bits of the P-code on each of the two L-band frequencies, measures the differential phase delay between L1 and L2, and uses this to estimate the total delay on L1. If D1 and D2 are the delays of the signal at L1 and L2, respectively, we have

$$D1 = (D2 - D1)/[(L1)^2 \bullet (1/(L2)^2 - 1/(L1)^2)].$$

Using the values above for L1 and L2, we obtain simply

$$D1 = (D2 - D1) \bullet 1.5457.$$

Thus, we measure (D2-D1) then solve for D1, the time delay of the L1 signal due to the ionosphere.

3. NIMS IMPLEMENTATION

We discuss here details of the design and operation of the receiver. Since the system is discussed in detail elsewhere [4], we simply summarize it here. The system uses a delay-and-multiply technique to recover the P-code clocks for all satellites in view. This contrasts with the CRL type receiver which uses a cross-correlation of the two L-band signals to directly measure the delay between the L-band channels. The NIMS, after recovering the sum of the P-code clocks for all satellites in view, then down-converts this composite signal to near base-band and passes eight-bit samples at 250 Hz to the software signal processor. The software uses the Doppler shifts and their rates of change to separate the different satellite signals, compute their phases coherently on both the L1 and L2 channels, and uses these differences to compute the ionospheric delay on the L1 channel, as

discussed above. We show block diagrams of the electronics, as well as discussing the functioning of the software.

Figure 1 shows the major elements of the NIMS in simplified form. The codeless technique recovers the 10.23 MHz P-code clocks for L1 and L2 through a delay-and-multiply operation [5,6,7]. Thus, we delay the signal by one-half of one chip of the 10.23 MHz code, and multiply this delayed signal by the direct signal. Narrow-band filtering this signal and converting to base-band produces a sine wave coherent with the clock driving the received P-code bits, without actually knowing the code. The signals from all satellites in view are contained as a sum of such sine waves with relative amplitudes and frequencies offset from each other by the Doppler shifts of the respective satellites.

These phases of the clocks of individual satellites are recovered in software by multiplying the composite signal by $\sin(j\omega t)$ and $\cos(j\omega t)$ and summing the sine and cosine components for 7.5 s. A 4 quadrant arctangent of these sums yields the clock phase. The frequency ω is near the base-band frequency of the receiver, 79 Hz, plus the Doppler shift. The Doppler shift, initially estimated from the GPS almanac, is accurately determined by using a second-order frequency-locked loop.

The receiver uses these phases for two purposes. First, the difference in phase between the L1 and L2 P-code clocks is used to determine the ionospheric delay on the L1 channel as discussed above. Measurement on L1 and L2 is carried out sequentially; that is, L1 is measured for 7.5 s followed by a 7.5 s measurement of L2. In addition, the phase difference from one L1 measurement to the next is used to compute frequency error in $(j\omega t)$ and close the tracking loop.

Sequentially measuring L1 and then L2 is analogous to the "tau-dither" loop in a GPS receiver and provides similar advantages and disadvantages. The major disadvantage is a degradation of the signal-to-noise (S/N) ratio by 3 dB. Advantages include greater simplicity and a resultant greater potential accuracy. Since the same narrow-band IF is used for both L1 and L2, the potential for errors due to unequal phase shifts through separate channels is minimized.

4. NIMS ACCURACY

A measure of the accuracy of the NIMS can be obtained from comparison with a system which determines ionospheric delay by observing the diurnal variation in Faraday rotation of the signal from the GOES-2 satellite. We computed the monthly mean

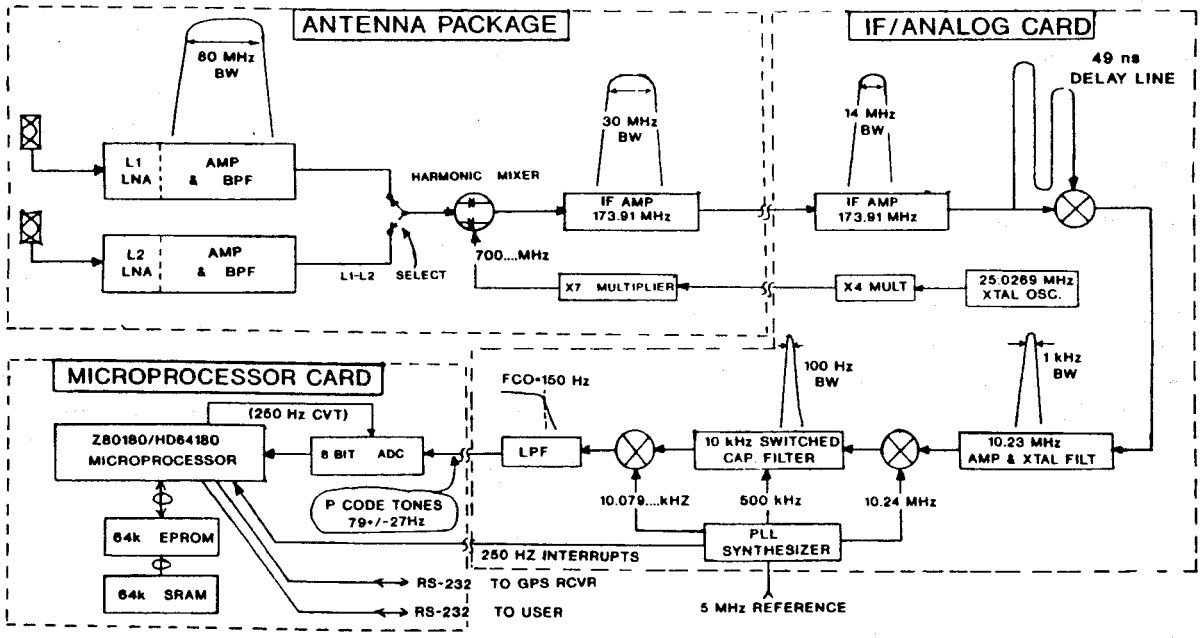

Figure 1- Block diagram of NIST Ionospheric Measurement System

diurnal variation of the vertical ionosphere using data from these two systems. From an analysis of the comparison of this mean for the months of December 1990 and June 1991, we deduce an agreement of the order of a few nanoseconds. However, there are a number of unknown variables involved with this comparison.

4.1 Monthly mean diurnal variations

The diurnal variation of the time delay of the 1.575 GHz signal can be expressed in terms of the equivalent delay of a signal traveling vertically through the ionosphere. This is achieved approximately by multiplying the observed delay by the cosine of the elevation angle E of the ray path. The approximate height of the centroid of the electron distribution is 400 km. In terms of the angle of elevation E at the ground, the vertical time delay Tv is obtained from the measured time delay Tm using

$$Tv = Tm \bullet \sqrt{1 - 0.89 \bullet \cos^2 \bullet E}.$$

The factor 0.89 is approximately the ratio squared of the earth's to the centroid of the electron distribution: $(6370/6770)^2$. To examine the monthly average diurnal variations of time delay, the 15 min linear fits of measurements of delays for every GPS satellite observed have been grouped into hourly means, that is, xx:30, xx:45, xx+1:00 and xx+15 delays have been averaged to yield the time delay for UT hour xx+1. Before averaging, data for angles of elevation less than 30° were removed in order to reduce errors caused by multi-path interference. Quarter-hourly linear fits for which the rms values are 6 ns and above have also been eliminated to improve the quality of the data. A few clearly inconsistent data were rejected by inspection.

The mean diurnal variation for February 1991 can be seen in Figure 2. The diurnal shape is in general agreement with the known characteristics of the ionosphere. There are two night minima, one near 6:00 UT the other near 12:00 UT, with an intervening maximum [1, section 8.6.7]. Noon and midnight in Boulder occur at 19:00 UT and 07:00 UT, respectively. The mean delay ranges from about 5 ns at night to 31 ns near noon. On individual days, delays will vary over a much larger range. For example, on January 30, 1991 the low value at 05:00 UT was 5.9 ns and the maximum at 20:00 UT was 38.2 ns.

4.2 Comparison between Ionospheric Delays from GPS and GOES-2

A measure of the total electron content of the ionosphere up to an altitude of about 2000 km can be obtained from measurements of the Faraday, or polarization, rotation of the electric field of a linearly polarized radio wave. Such signals, emitted from the GOES-2 synchronous equatorial satellite located near 59° W, have been measured, and some sample diurnal comparisons are shown in Figures 2 and 3 for a winter and summer month, respectively. The comparison is only for those hours for which measurements were available for both GPS and GOES-2.

In June, the shapes of the GPS and GOES-2 curves are similar, with the GPS delays consistently higher than those for GOES-2. This is to be expected because the Faraday data are weighted by the geomagnetic field, which diminishes with altitude, and give the content up to a height of about 2000 km. On the other hand, the GPS time delays are unaffected by the geomagnetic field and they yield ionospheric electron contents up to the height of the satellite (20,000 km).

Reliable measurements of the difference between the total electron content and the Faraday content, called the protonospheric content, are few. The best measurements were made around solar minimum 1974-1976 [9] using the ATS6 radio beacon. In the USA in summer, the mean protonospheric content shows little diurnal variation and is about 10% of the midday content. On winter nights the protonospheric content is about half of the total content.

Diurnal variations of GPS and GOES-2 delays for a winter month are shown in Figure 2. There is a marked difference from the June 1991 behavior in that while the afternoon and evening GPS delays are greater than the corresponding GOES-2 delays the reverse is true from sunrise to early afternoon. These differences almost certainly reflect geographical differences in the ionosphere. The maximum ground distance involved is about 1200 km which applies to an altitude of 400 km and when 2 satellites are at elevations of 30° in a great circle plane.

While the GPS data nominally refer to Boulder (40° N, 105° W) the GOES-2 data refer to the sub-ionosphere point near 36.2° N, 97.9° W. The longitude difference is equivalent to a local time difference of 28.4 min. The method of obtaining the

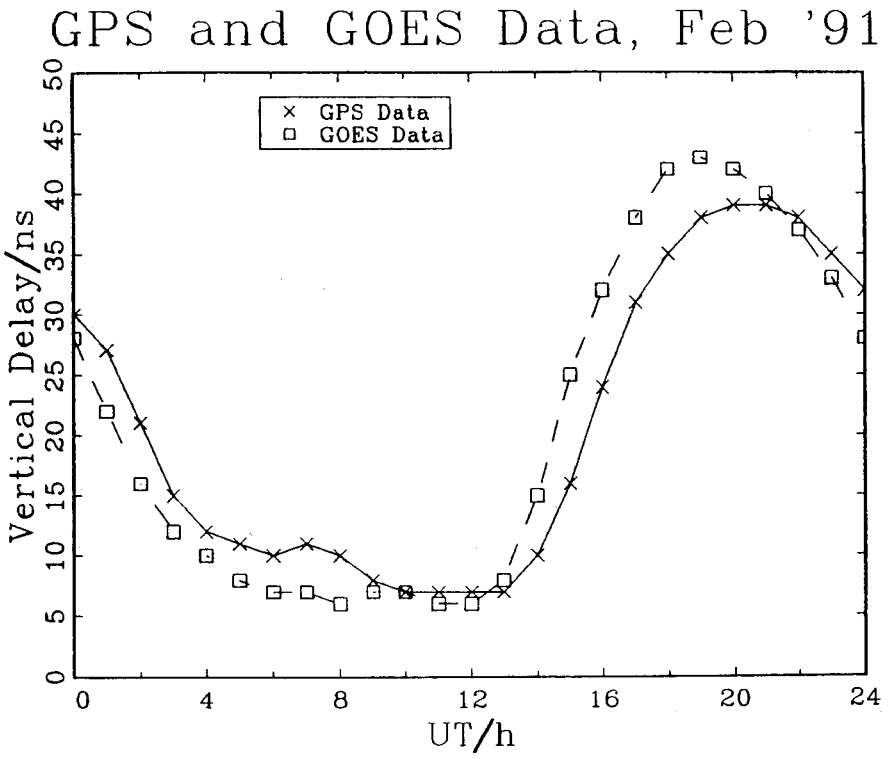

Figure 2. Comparison of the equivalent vertical ionospheric delays on 1.575 GHz from GPS and from Faraday rotation on 136.38 MHz from GOES-2 synchronous satellite at 59° W, received at Boulder in a summer month.

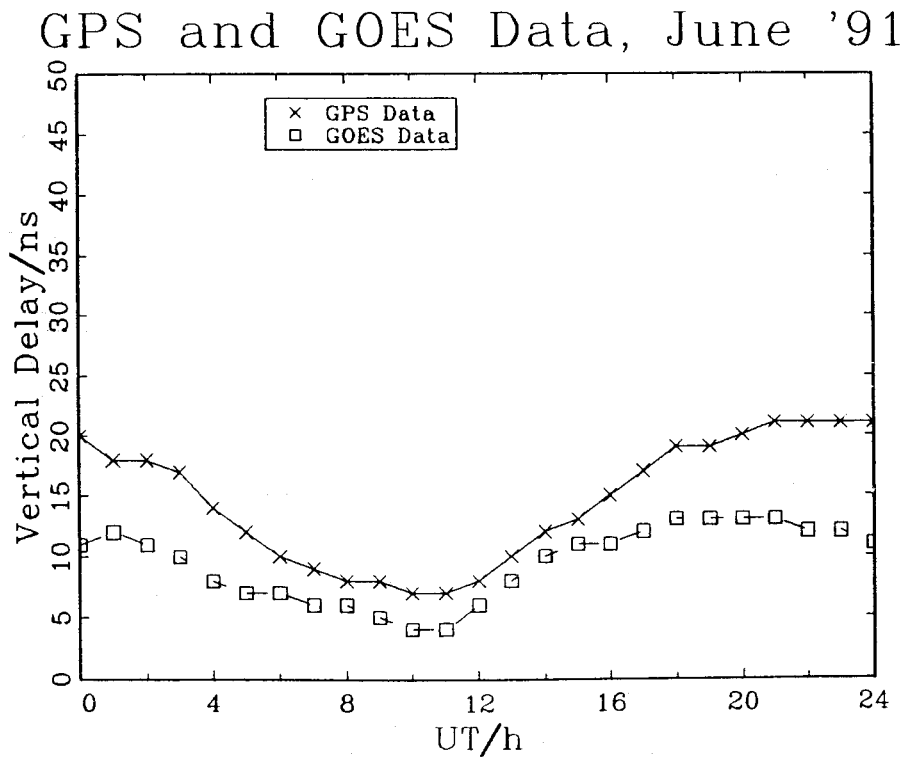

Figure 3. Comparison of the equivalent vertical delays on 1.575 GHz from GPS and from FAraday rotation of 136.38 MHz signals from GOES-2 received in Boulder in a winter month.

hourly mean leads to a time shift of around -7.5 min, so a positive time shift of 36 min should be applied to the GOES-2 curve in Figure 2. Such a time shift reduces the morning-noon discrepancy but does not eliminate it. The GOES-2 noon delay is certainly greater than the GPS noon delay and this indicates that the electron content decreases with increase of latitude, that is, with increase of solar zenith angle, as would be expected. Assuming that the protonospheric delay is 10% of the noon Faraday (43 ns), the total delay up to the satellite should be around 47 ns. This is considerably larger than the GPS delay of 39 ns. Similar situations hold in December 1990 and in January 1991.

During December 1990 and January 1991, the nighttime minima obtained with both GPS and GOES-2 are close. From the ATS6 experience we anticipate that the GPS delay would be about twice that of the GOES-2 delay. This suggests that the GPS delays should be increased by approximately 5 ns. This additional delay ensures that the maximum diurnal GPS delays exceed the maximum GOES-2 delays for all months except February 1991. Unfortunately, this makes the summer GPS maximum delay twice that of the corresponding GOES-2 delays. This large summer discrepancy indicates that real geographical differences exist and are appreciable.

4.3 Uncertainties in Faraday Rotation Measurements

The GOES-2 Faraday technique suffers from the disadvantage of an unknown orientation of the satellite antenna, therefore, the direction of the electric field in the absence of the ionosphere is not known. A minimum error is zero and a maximum error is +/- 1.2 ns. An additional error is the cycle ambiguity. The number of cycles in the total polarization has to be determined at night by inspection. This is aided by measurements, at Boulder, of the maximum electron density and suitable models of the thickness of the ionosphere obtained from a long-term data base. At night the ambiguity could be +/- 2.4 ns but, during daytime errors of several cycles are possible when there is a break in the continuity of the rotation record.

4.4 Uncertainties in NIMS Measurements

There are several sources of inaccuracies in the NIMS data. We consider: (a) the phase (or time) differences between the signals on the two frequencies (1227.6 GHz and 1.575 GHz), (b) delays in the receiving system, (c) temperature changes in the receiving system (d) multi-path interference, and (e) interference between received signals when the Doppler shifts used for discrimination are nearly equal. We discuss most of these at length in the sections on the NIMS data, but we will mention here some information about (a) and (c).

In general the delays in the space vehicles are unknown. The differential delay between the 1.2 GHz and 1.5 GHz channels produces a "bias" in the delay measurements. Reference [10] gives biases for some space vehicles. These biases vary from -0.5 ns to 14 ns. The extent to which these biases vary over the long term is unknown. In the present work no allowance has been made for these biases, and, hence, there is a net error in the GPS time delays. The net effect on the equivalent vertical time delay will depend on the space vehicles involved and their elevation angles.

We performed an experiment to determine the temperature dependence of the NIMS antenna in 1989. We used a signal generator attached to the antenna package of units #101 and #102 to simulate the signal coming from the antenna. Each antenna package was placed in an environmental chamber and cycled from -20 to +50°C while continuous measurements of L1 delay were made. The measured L1 bias changed by less than 2 ns over this temperature range on both units, as shown in Figure 4. These measurements do not characterize the change in delay of the volute antennas; however their contribution to the delay instability should be small compared to the that of the bandpass filters.

5. THE STABILITY OF THE NIMS DATA

5.1 The 15 Second Measurements

We will use a recently developed statistical tool, the time variance or TVAR [11], to look at the 15 s measurements. TVAR is computed by multiplying the integration time τ times the modified Allan variance divided by $\sqrt{3}$. White phase noise is characterized by a $\tau^{-1/2}$ dependence, causing a slope of -½ in a log-log plot. A parabolic curve causes a slope of +2. For white phase noise, TVAR gives the classical standard deviation at τ_0, the minimum τ, and the standard deviation of the mean for τ equal to the data length.

Figures 5b and 6b are TVAR plots of 15 s data for PRN's 2 and 19, respectively. Each plot is the rms of variances computed from several days. We see that the stability of the ionospheric measurements is

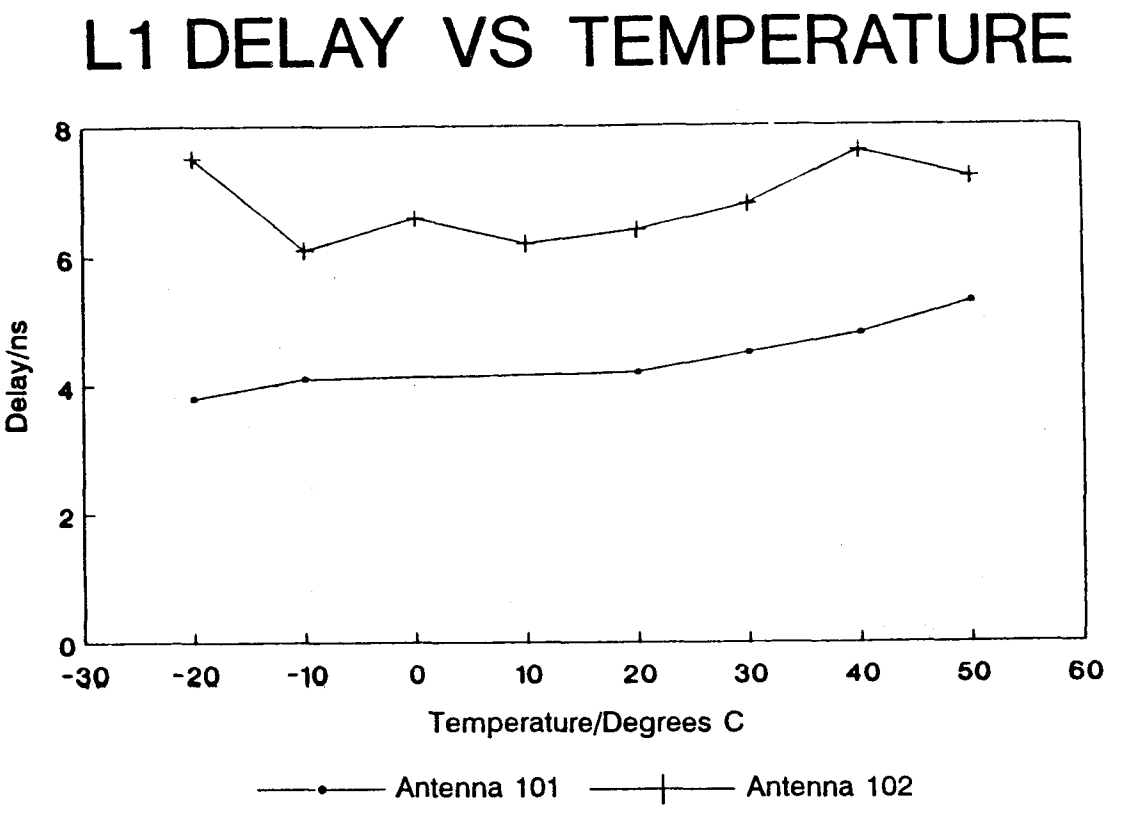

Figure 4. Measured delay bias vs. temperature for two NIMS antenna packages.

1 ns at 15 s integration time and continues to average as white noise out to about 16 min, though the bulge above the -½ slope from about 4 to 16 min of integration appears to be sinusoidal modulation. We conclude from this and from other analyses that the noise in the 15 s measurements of the ionospheric delay is typically less than about 1 ns. The white phase modulation we see out to about 16 min we interpret as fluctuations of the ionosphere itself. The sinusoidal modulation from 4 to 16 min we believe to be due to multi-path interference.

Figures 5a and 6a show the actual 15 s data for PRN's 2 and 19, which were used to compute TVAR in Figures 5b and 6b. Each figure shows several days of data plotted on top of each other. We can see the large scale structure, the change in ionospheric delay, that largely repeats each day. Also visible in both plots is a short period where the noise increases markedly. These are periods where the Doppler offset of that satellite comes within about 1 Hz of another. This effect forms as follows. The signals from all the satellites are present as a sum in one channel in the NIMS. Since the Doppler offsets are used to identify the satellites and track them, when two satellites have a similar offset it is difficult to separate their signals. The NIMS integrates measurements for 7.5 s before it actually computes the phase of the P-code clock of the signal. If two Doppler shifts are 1 Hz apart, the noise from one will appear in the measurement of the other as a sin(t)/t curve with nulls at the period of the Doppler offset, 1 s in this case. This pulls the software second-order frequency locked loop and biases the measurements. Each satellite typically experiences this once or twice in each pass, for a time interval up to a few min. The 15 min linear fits of the 15 s data retain only small effects from this, typically increasing the rms of the fit to about 4 ns, and biasing the data by under 2 ns.

Also, Figures 5a and 6a show small fluctuations which repeat each day, especially toward the beginning and end of the track when the satellite is at a low elevation. These are probably multi-path deviations [12]. Visually, they appear to be as large as 5-10 ns. These are probably the effects which cause the "bumps" in the TVAR plots, Figures 5b and 6b discussed above.

5.2 The 15 Minute Data

The NIMS does a linear fit to the 15 s data every 15 min and stores this data for retrieval by modem.

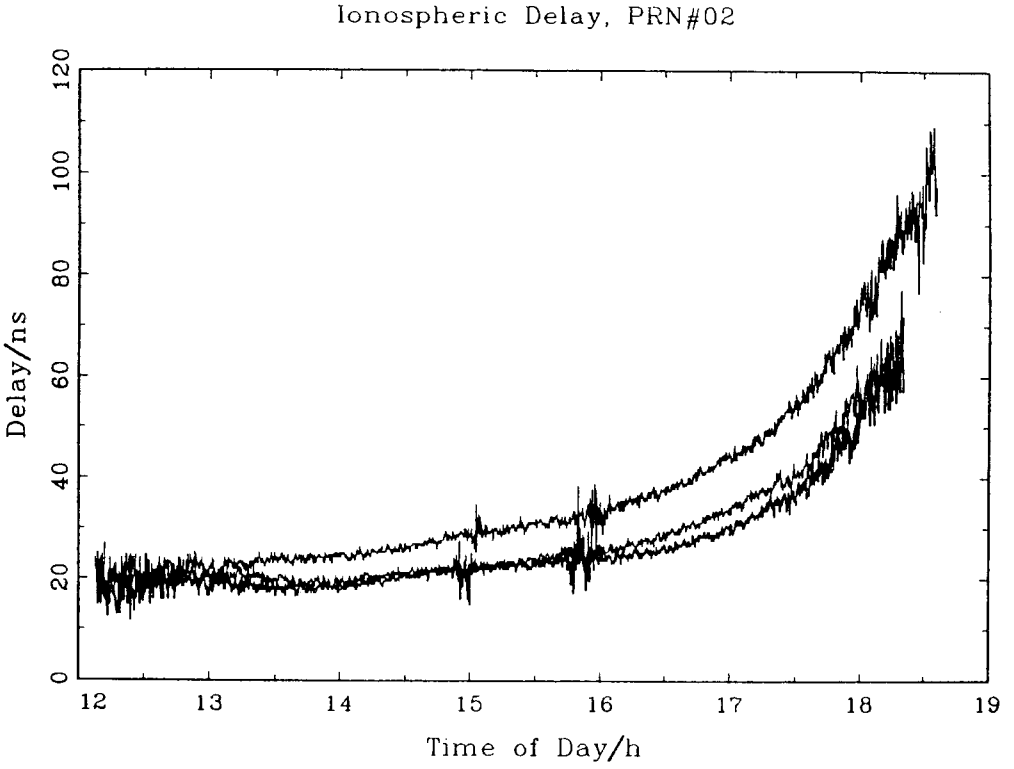

Figure 5a. Consecutive days of 15 s data from PRN#2.

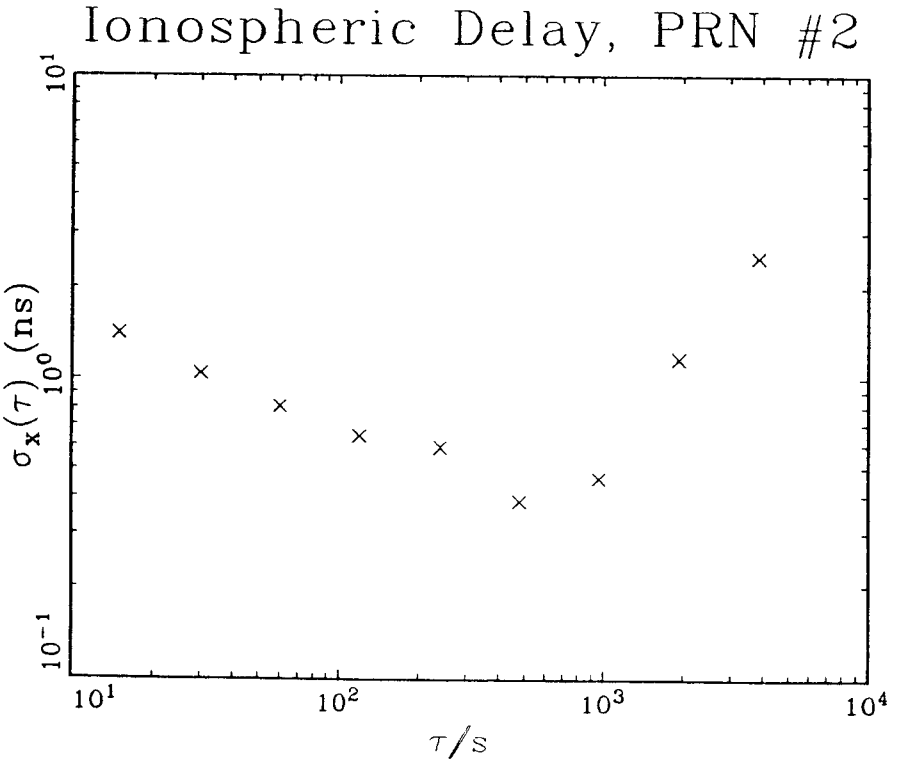

Figure 5b. The RMS TVAR for the data in figure 5a, PRN#2.

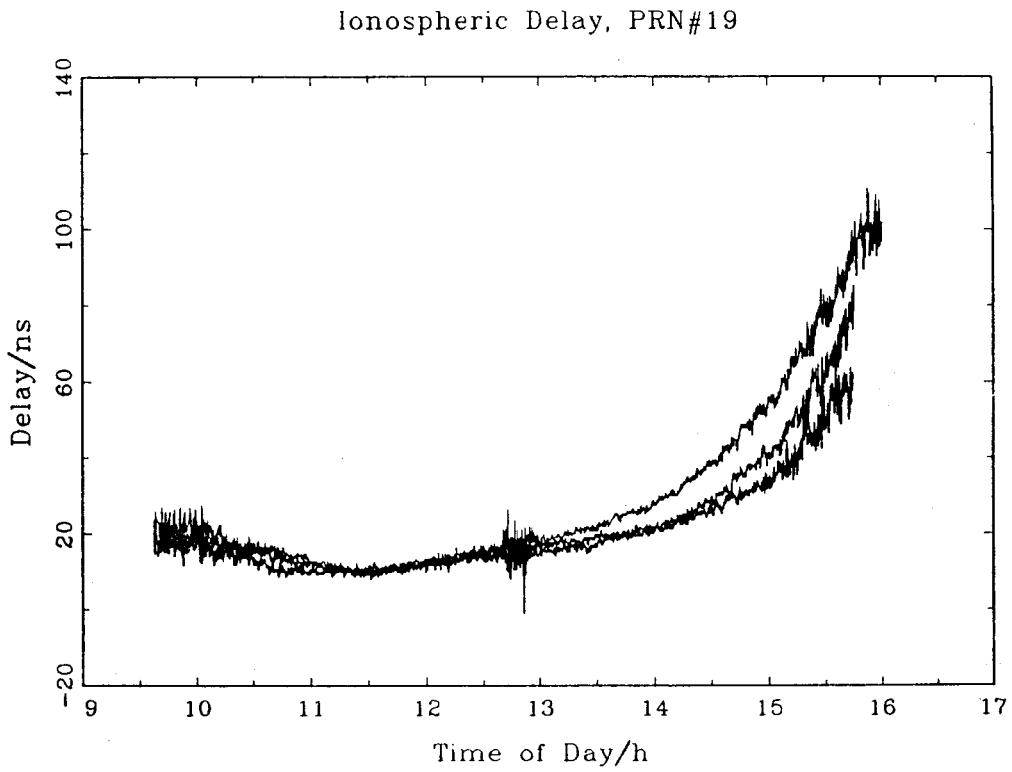

Figure 6a. Consecutive days of 15 s data from PRN# 19.

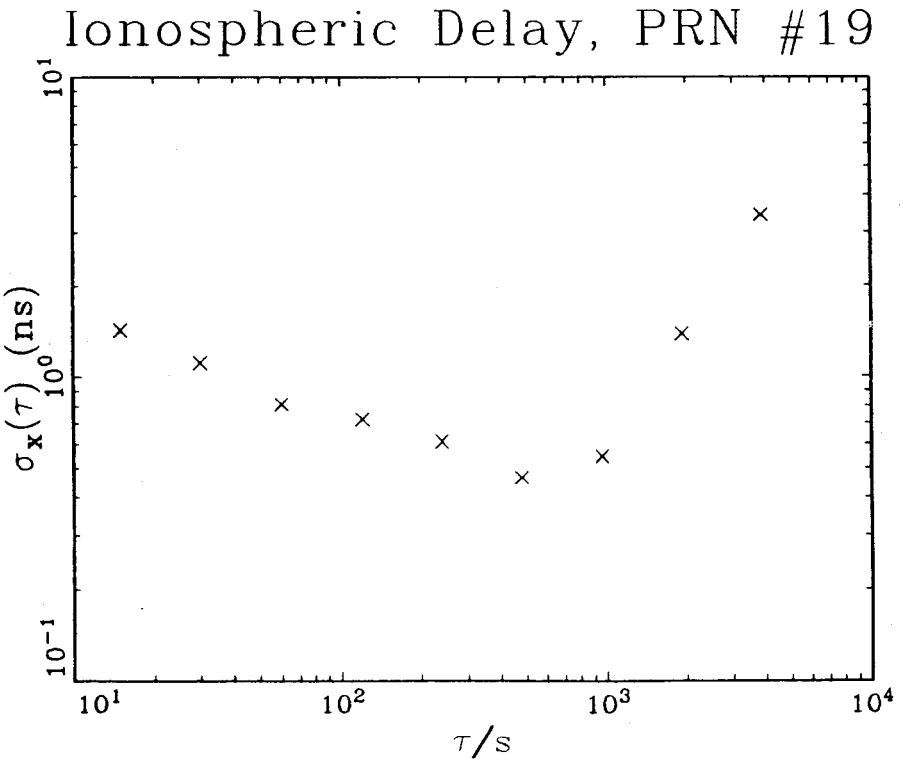

Figure 6b. The RMS TVAR for the data in figue 6a, PRN# 19.

Since the fluctuations are white, except for multi-path interference, out to 15 min, as we saw in the previous section, we lose little information this way and we average out multi-path interference. We will look at the equivalent vertical delay of these 15 min points, as well as a comparison of 15 min values between two NIMS's. From these we draw conclusions about the stability and accuracy of the measurements.

Figure 7 shows the vertical ionospheric delay computed using all satellites over a 10 d period starting MJD 48493, that is, August 25, 1991. We have plotted all individual 15 min points for all satellites tracked above 30° elevation, for which the rms of the linear fit was less than 7. Since the receiver locks on many satellites at once, the spread of ionospheric measurements at a given time appears as a vertical line. As we discussed previously, this could be due to several causes. One cause is that the equivalent point of intersection of the signal with the ionosphere varies over a spatial range; hence there are real differences for the vertical delay at a given time. A second possible cause is that different satellites give different biases in the ionospheric measurements due to different fixed offsets of the P-code between their L1 and L2 channels. Also, different multi-path interference between satellites could cause different measured delays.

To sort out these possibilities let us look at the variation in the nighttime ionosphere. We see a maximum variation at a given time of about 8 ns. This provides an upper limit to variations caused by either differing offsets of the P-code between the L1-L2 channels, or by multi-path interference, since both of these effects are independent of the total delay through the ionosphere. Either of these effects could cause an 8 ns variation. In the section above we saw multi-path deviations of the order of 5-10 ns at low elevation angles. Coster et. al. [10] has shown L1-L2 biases varying among satellites from -0.5 to 14 ns. We then conclude from this that the larger variations which occur when the vertical ionosphere is thicker are due to spatial differences in the location of the point of intersection of the satellite signal with the ionosphere.

Figure 8 shows the differences between the measured delays of two NIMS's at NIST, #110 and #114, over the same period as the data above. The delay of unit #114 was not calibrated, and the bias correction was set at 0. Surprisingly, we see a clear a diurnal effect correlated with the vertical delay. The change in the mean seems visually of the order of 2-3 ns. At this time we have not found a mechanism that could cause this. Overall, the mean of the difference is 6.8 ns (due to having no bias correction), with a standard deviation of 1.5 ns.

Biases in the NIMS are not a significant problem for differential time transfer as long as the value indeed remains constant. In fact, the L1-L2 delay biases in the SV's are also not a problem, since in common-view time transfer, we are looking at the same SV, and any bias within the SV will be common to all participating users, and will drop out when the differences of the time transfer measurements are taken.

5.3 Predictability of the Ionosphere

We study here the predictability of the NIMS measurements for use in correcting GPS time data. For this purpose we look at a period of high fluctuation. There was a large solar magnetic storm around June 5, 1991, MJD 48412. Figure 9 shows the vertical ionospheric delay for a 10 d period around this event. The large increase in vertical delay during the magnetic storm is apparent. We use these data to give us a worst-case scenario for studying the use of quadratic fits to NIMS data to estimate ionospheric delay at specific times.

We select a set of 15 min measurements in different ways and use these to predict another measurement. In this way, we estimate the error in correcting the GPS time measurements with quadratic fits of NIMS data. This is necessary when we do not have an ionospheric measurement coinciding with a GPS time measurement. It is also sometimes desirable to smooth a 15 min measurement with neighboring data. We either estimate the delay at a time contained within an interval of measurements, or we predict a 15 min measurement using its neighbor.

For estimating the delay at a time contained within an interval of measurements, we pick an interval in one of two ways. In either case we use three points to estimate a fourth which they temporally surround. In the first case we take four consecutive 15 min measurements (spanning 1 h) and use three of them to estimate one of the interior ones. In the second case, we expand this interval, taking four measurements spanning 1.25 h, and pick three of them to estimate one of the middle one. This looks like:

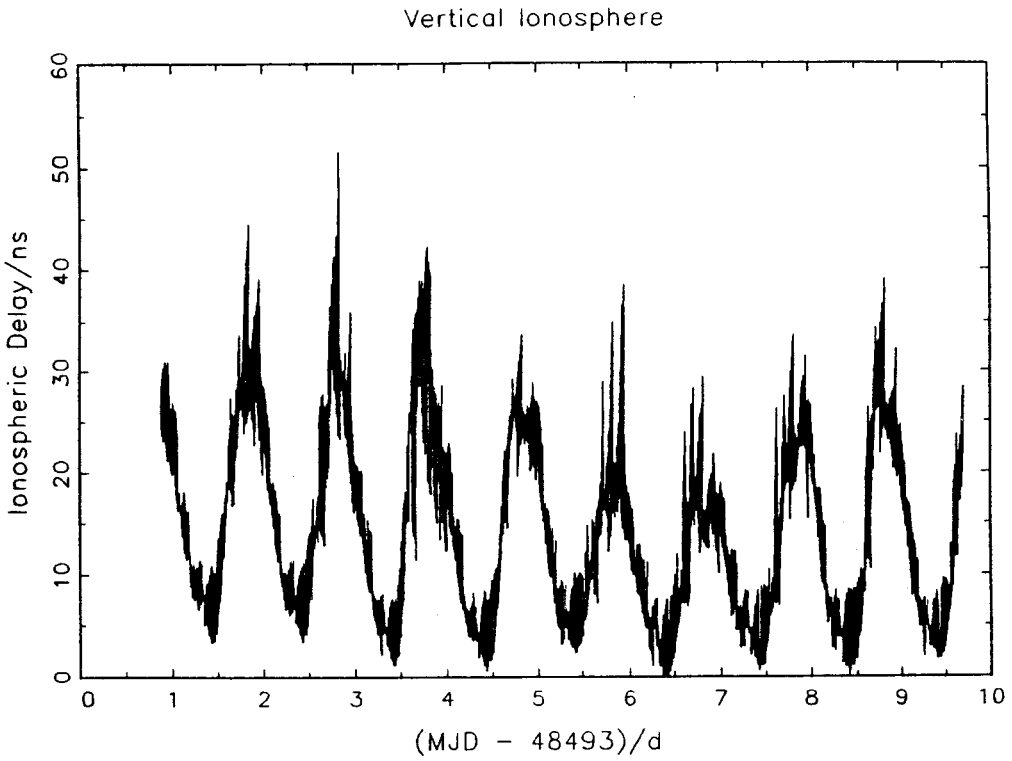

Figure 7. The equivalen vertical delay for each 15 min linear fit for all satellites above 30° elevation. Fits with rms $\geq$ 7 ns have been omitted.

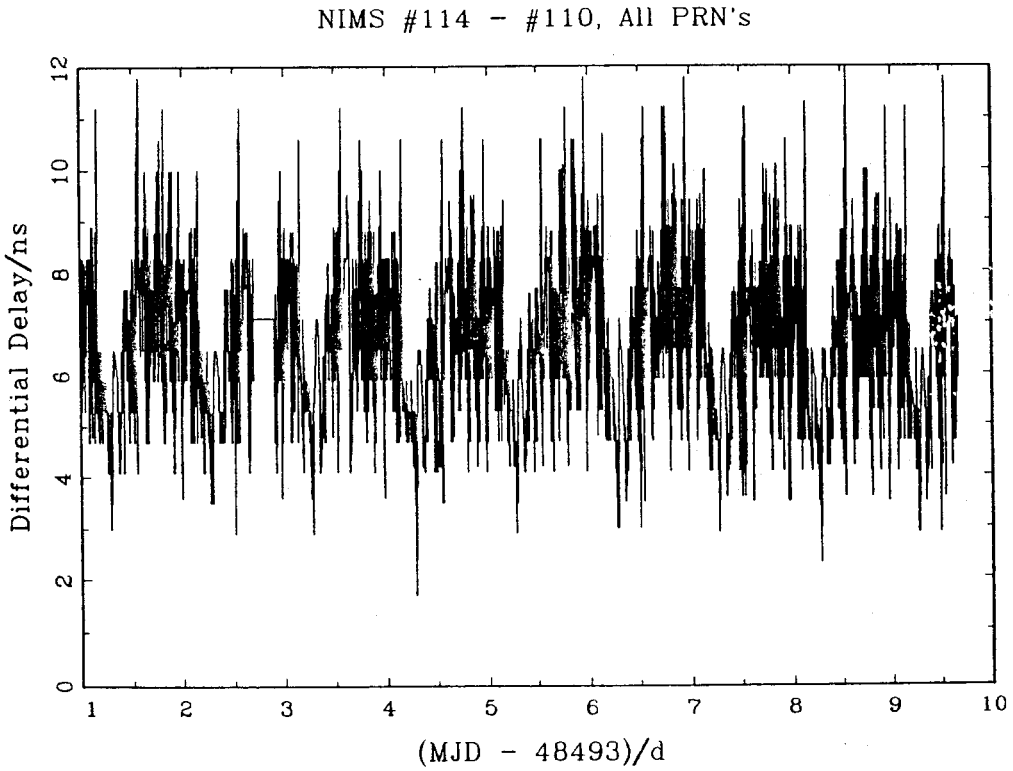

Figure 8. Differential delay for NIMS #114 - NIMS #110, showing the delay bias of NIMS #114.

	Case 1			
Time in minutes:	t	t+15	t+30	+45
Data:	X_1	X_2	X_3	X_4

We either estimate X_2 with X_1, X_3, and X_4, or we estimate X_3 with X_1, X_2, and X_4.

	Case 2a				
Time in minutes:	t	t+15	t+30	t+45	t+60
Data:	X_1	not used	X_2	X_3	X_4

We estimate X_2 with X_1, X_3, and X_4.

	Case 2b				
Time in minutes:	t	t+15	t+30	t+45	t+60
Data:	X_1	X_2	X_3	not used	X_4

We estimate X_3 with X_1, X_2, and X_4.

Using a TVAR analysis, we found that the estimate-measurement residuals averaged to a mean faster than white noise, thus the mean and standard deviation of the mean are defined. We summarize our results in Table 1.

Table 1

	Mean Prediction Error	Standard Deviation
Case 1	-0.2 ns	0.9 ns
Case 2	-0.2 ns	2.2 ns

We also used the slope and intercept of one 15 min linear fit to extrapolate to the midpoint of its neighbor. This is important since GPS tracks for intercontinental common-view measurements often have low elevation angles and are more difficult for the NIMS to track. Thus there are cases where the NIMS will complete a measurement 15 min after the GPS track. For this reason we are particularly interested in low angle cases. We looked over the 10 d including the magnetic storm, extrapolating one measurement from its neighbor for all satellites. When we specifically selected tracks with an elevation below 30°, the results were a mean of -0.4 ns, and a standard deviation of 2.7 ns. In most cases this extrapolation should be an improvement over the ionospheric model which is broadcast from the GPS satellites.

6. CLOSURE AROUND THE WORLD

Typically, in GPS time transfer the four principal error sources are the local antenna coordinates, the broadcast ionospheric model, the broadcast ephemerides, and multi-path interference. Some receivers also contribute significant delay variations. Previous work shows the impact of correcting the coordinates, the ionospheric model, and the broadcast ephemerides individually [13,14,15]. The gain in precision for long-distance time comparisons when two common-view links are corrected with measured ionospheric values [16] has already been shown. The gain in accuracy was also pointed out in a study of the closure around the world using NIST, OP, and CRL [14,17]. We show the implications of this work for the accuracy of the NIMS, where the data set has been extended. We present here a 273 d experiment where three long-distance time links are performed with simultaneous reduction of these error sources. The laboratories involved are the Paris Observatory (OP), Paris, France; the National Institute of Standards and Technology (NIST), Boulder, Colorado, USA; and the Communications Research Laboratory (CRL), Tokyo, Japan. The closure around the world was then obtained by combination of these time links. Since the closure should add to 0, we have a clear test of accuracy of the overall GPS time transfer. The accuracy of the NIMS, of course, contributes to this, and the number sets an upper bound.

6.1 Experiment

The three long-distance time transfers UTC(OP)-UTC(NIST), UTC(NIST)-UTC(CRL) and UTC(CRL)-UTC(OP) were computed using the common-view method [18], for a 273 d period, from 1990 June 16 (MJD 48058) to 1991 March 16 (MJD 48331). The GPS data were taken at the three sites corresponding to international tracking schedules issued by the BIPM. The time comparison values UTC(Lab1)-UTC(Lab2) were obtained for each observed satellite at the time Tmid of the midpoint of the track.

6.2 Measured Ionospheric Delay

The GPS receivers automatically correct for the ionospheric refraction using a model [19] whose parameters are broadcast in the GPS C/A message. We use here two types of codeless systems, the NIMS and the CRL type receiver developed by M. Imae [20], to improve upon this model.

We estimated the value of the measured ionospheric delay for a given 13 min track by interpolating from measurements. For this, we used several ionospheric measurements for the same satellite, surrounding the time at the midpoint of the 13 min track, Tmid. A polynomial fit was then computed (linear or cubic depending on the number of values which are used). The estimated value was deduced for Tmid by interpolation and used to correct UTC(Lab) - GPS time. This polynomial fit was never extrapolated and measurements from other satellites were never used.

6.3 Precise Ephemerides

The GPS precise ephemerides were computed at the U.S. Naval Surface Warfare Center (NSWC) from the beginning of 1986 to 1989 July 29. Since then they have been produced by the Defense Mapping Agency (DMA). They were applied by recomputing the satellite position using the ephemeris broadcast during the track, comparing this position with that estimated from the precise ephemeris, and projecting this difference vector onto the direction vector from the receiver location to the satellite. Detailed results of this work are reported elsewhere [21].

6.4 Results

Four different cases are emphasized in this study:

* uncorrected values,
* values corrected for ephemerides only,
* values corrected for ionosphere only,
* values corrected for both ephemerides and ionosphere.

For each of these four cases, a Vondrak smoothing [22] was performed on the values UTC(Lab1) - UTC(Lab2). The smoothing used acted as a low-pass filter with a cut-off period of about 3 d.

A TVAR analysis, Figure 10, allows us to characterize the noise processes of the closure. For periods less than 4 d, we see the effects of the smoothing. With uncorrected data the closure exhibits flicker phase noise. When corrections are applied, the flicker phase noise drops, and with the precise ephemeris correction, the noise type after 4 d appears to be white phase noise. It is then justified to compute mean values and their standard deviations of the closure for a 20 d period. Table 3 gives these results.

We find some indication here that the precise ephemeris removes the flicker phase noise, thus reducing the biases and leaving white phase noise, while the measured ionospheric corrections lower the overall noise. The standard deviation of the mean over 20 d, ($\sigma_x(\tau=20d)$), is about 1 ns.

TABLE 3: Mean values of the closure around the world estimated by the quantity [UTC(OP) - UTC(NIST)] + [UTC(NIST) - UTC(CRL)] + [UTC(CRL) - UTC(OP)] and standard deviations.

averaging	Precise Ephemeris		Prec. Eph. + Meas. Iono.	
period	Mean	Std. Dev.	Mean	Std. Dev.
48059-48078	16.1	8.78	7.59	3.32
48079-48098	21.9	5.11	8.50	2.19
48099-48118	11.1	6.03	4.76	3.50
48119-48138	29.3	5.95	2.01	2.32
48139-48158	26.6	5.66	4.49	4.20
48159-48178	20.0	6.61	3.99	4.33
48179-48198	17.5	2.94	4.28	2.35
48199-48218	8.37	3.60	3.51	3.59
48219-48238	1.98	6.11	8.98	4.22
48239-48258	-2.71	7.52	4.04	2.77
48259-48278	-7.89	7.39	3.03	4.15
48279-48298	-8.39	5.52	6.60	3.46
48299-48318	-7.12	6.41	5.19	3.09

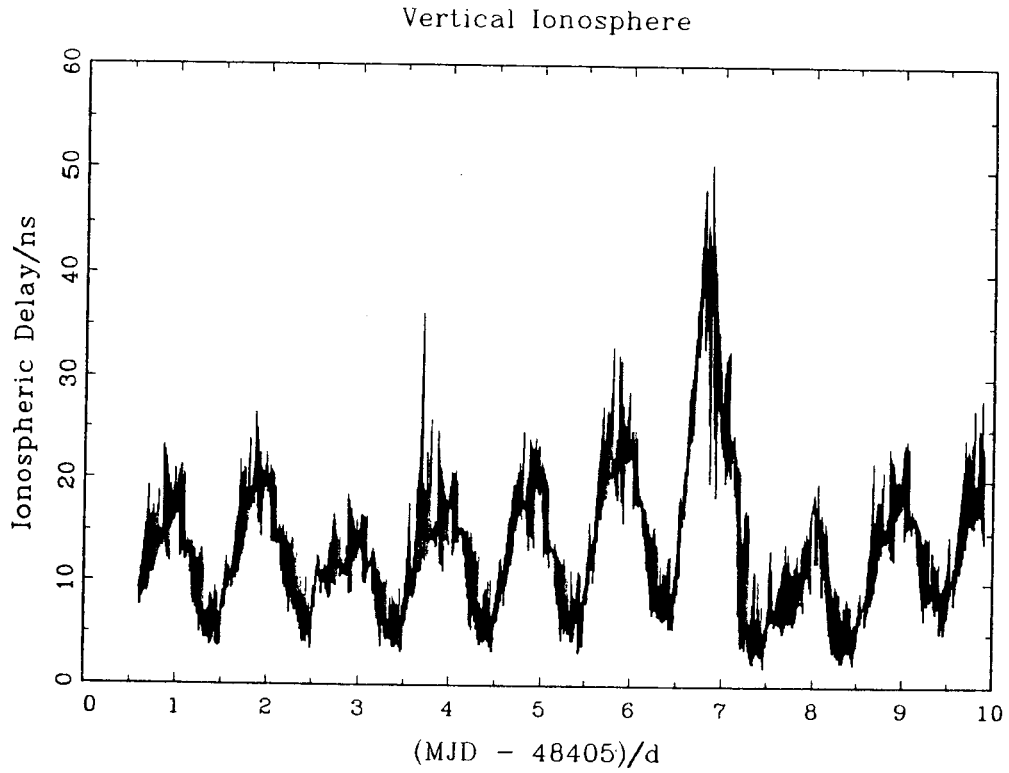

Figure 9. The equivalent vertical delay for a period containing a magnetic storm. As in Figure 7, we have each 15 min linear fits for all satellites above 30° elevation. Fits with rms >= 7 ns have been omitted.

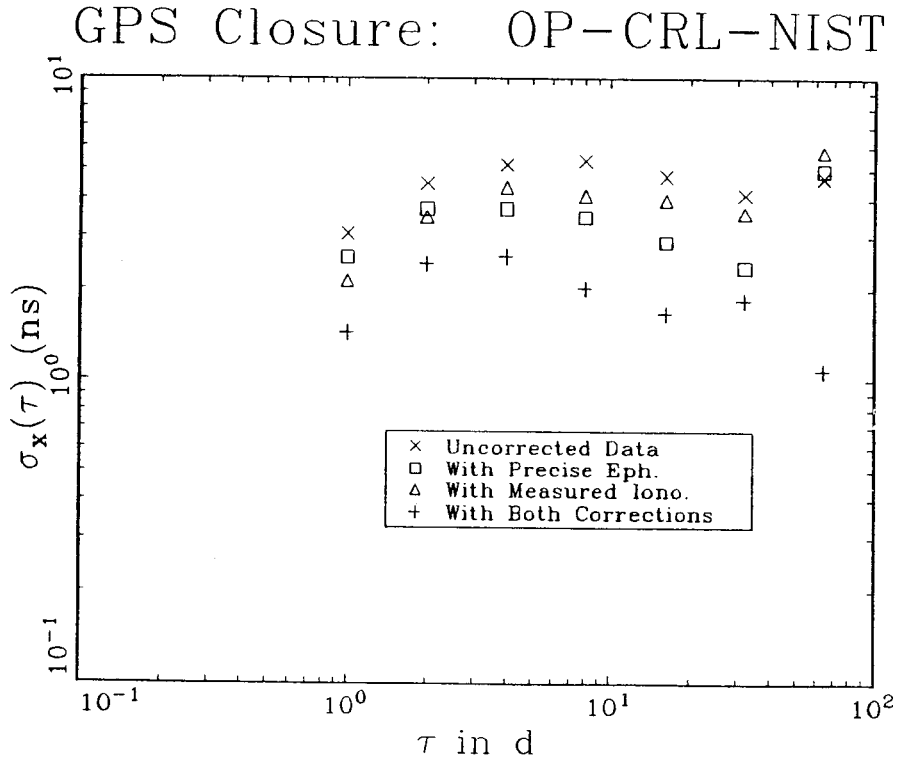

Figure 10. The time variance of the GPS common-view time transfer closure around the world. Consisting of: UTC(OP)-UTC(NIST) + UTC(CRL)-UTC(OP) + UTC(NIST)-UTC(CRL). We have uncorrected data, data corrected with the precise ephemeris, data corrected with measured ionospheric delays, and data with both corrections.

REFERENCES

[1] K. Davies, Ionospheric Radio, P. Peregrinus Ltd., London, U.K., 1990.

[2] D. W. Allan, D. D. Davis, M. A. Weiss, A. Clements, B. Guinot, M. Granveaud, K. Dorenwendt, B. Fischer, P. Hetzel, S. Aoki, M. K. Fujimoto, L. Charron, N. Ashby, "Accuracy of International Time and Frequency Comparisons via Global Positioning System Satellites in Common-View," IEEE Trans. Instrum. Meas., vol IM-34, pp.118-125, 1985.

[3] M. A. Weiss, D. W. Allan, "An NBS Calibration Procedure for Providing Time and Frequency at a Remote Site by Weighting and Smoothing of GPS Common View Data," IEEE Trans. IM., Vol IM-36, No.2, pp 572-579 (June, 1987).

[4] D. Davis, M. A. Weiss and M. Vidmar, "A codeless ionospheric calibrator for time transfer applications," Proc. of the Institute of Navigation Satellite Division,
2nd International Technical Meeting (ION GPS-89), 1989.

[5] MacDoran et al., "SERIES: Satellite Emission Range Inferred Earth Surveying," Proceedings of the Third International Symposium on Satellite Doppler Positioning. New Mexico State University (February 1982) 1143-1164.

[6] MacDoran et al., U S Patent 4,797,677 Jan 10, 1989.

[7] R. Bruce Crow et al., "SERIES-X Final Engineering Report" JPL D-1476 Jet Propulsion Laboratory, Pasadena California (August 1984).

[8] M. Imae et al., "A DUAL Frequency GPS Receiver Measuring Ionospheric Effects without Code Demodulation and its Application to Time Comparisons," Proc. of the Twentieth Annual Precise Time and Time Interval (PTTI) Applications and Planning Meeting, Nov. 29-Dec. 1, 1988, pp. 77-85.

[9] K. Davies, "Recent progress in satellite radio beacon studies with particular emphasis on the ATS-6 radio beacon experiment," Space Sci. Rev. vol. 25, p. 357, 1980.

[10] A.J. Coster, E.M. Gaposchkin, L.E. Thornton, M. Buonsanto and D. Tetenbaum, "Comparison of GPS and incoherent scatter measurements of the total electron content," The Effect of the Ionosphere on Radiowave Signals and System Performance, ed. J.M.Goodman, Naval Research Laboratory, Washington. D.C. p 460, 1990.

[11] D. W. Allan, M. A. Weiss, J. L. Jespersen, "A Frequency-Domain View of Time-Domain Characterization of Clocks and Time and Frequency Distribution Systems," Proc. 45th Annual Symposium on Frequency Control, 1991.

[12] G. J. Bishop and J. A. Klobuchar "Multipath effects on the determination of absolute ionospheric time delay from GPS signals" Radio Science, vol. 20, pp. 388-396 (May-June 1985).

[13] B. Guinot and W. Lewandowski, "Improvement of the GPS time comparisons by simultaneous relative positioning of the receiver antennas," Bulletin Geodesique, vol. 63, pp. 371-386, 1989.

[14] M. A. Weiss, T. Weissert, C. Thomas, M. Imae and K. Davies, "The use of ionospheric data in GPS time transfer," Proc. 4th European Frequency and Time Forum, pp. 327-333, 1990.

[15] W. Lewandowski and M. A. Weiss, "The use of precise ephemerides for GPS time transfer," Proc. 21st Annual Precise Time and Time Interval (PTTI) Applications and Planning Meeting, pp. 95-106, 1989.

[16] M. Imae, M. Miranian, W. Lewandowski and C. Thomas, "A dual-frequency codeless GPS receiver measuring ionospheric effects and its application to time comparison between Europe and USA," Proc. 3rd European Frequency and Time Forum, pp. 89-93,1989.

[17] W. Lewandowski, G. Petit, C. Thomas, M.A. Weiss, "GPS Time Closure Around the World Using Precise Ephemerides, Ionospheric Measurements, and Accurate Antenna Coordinates," Proc. 5th European Frequency and Time Forum, 1991.

[18] D. W. Allan and M. A. Weiss, "Accurate time and frequency transfer during common-view of a GPS satellite," Proc. 34th Annual Symposium on Frequency Control, pp. 334-346, 1980.

[19] J. A. Klobuchar, "Ionospheric correction for the single frequency users of the Global Positioning System," IEEE Trans. NTS, 1982.

[20] M. Imae, W. Lewandowski, C. Thomas and C. Miki, "A dual-frequency GPS receiver measuring ionospheric effects without code demodulation and its application to time comparisons," Proc. 20th Annual Precise Time and Time Interval (PTTI) Applications and Planning Meeting, pp. 77-86, 1988.

[21] W. Lewandowski, G. Petit, C. Thomas and M. A. Weiss, "The use of precise ephemerides, ionospheric data and corrected antenna coordinates in a long-distance GPS time transfer," Proc. 22nd Annual Precise Time and Time Interval (PTTI) Application and Planning Meeting, 1990.

[22] J. Vondrak, Bull. Astron. Inst. Czechoslovakia, vol. 20, p. 349, 1969.